MULTIDIMENSIONAL QUANTUM TUNNELLING FORMULATION OF OXYGEN-16 AND URANIUM-238 REACTION

A THESIS SUBMITTED TO
THE GRADUATE SCHOOL OF NATURAL AND APPLIED SCIENCES
OF
MIDDLE EAST TECHNICAL UNIVERSITY

BY

MURAT TAMER ATAOL

IN PARTIAL FULFILLMENT OF THE REQUIREMENTS FOR THE DEGREE OF

MASTER OF SCIENCE

IN

PHYSICS

JUNE 2004

Approval of the Graduate School of Natural and Applied Sciences.

Prof. Dr. Canan Özgen
Director

I certify that this thesis satisfies all the requirements as a thesis for the degree of Master of Science.

Prof. Dr. Sinan Bilikmen
Head of Department

This is to certify that we have read this thesis and that in our opinion it is fully adequate, in scope and quality, as a thesis for the degree of Master of Science.

Prof.Dr. Şakir Ayık
Co-Supervisor

Prof. Dr. Osman Yılmaz
Supervisor

Examining Committee Members

Prof. Dr. Mehmet Abak (HU, PHYS) _____

Prof. Dr. Osman Yılmaz (METU, PHYS) _____

Prof. Dr. Cüneyt Can (METU, PHYS) _____

Prof. Dr. Ahmet Gökalp (METU, PHYS) _____

Assoc. Prof. Dr. Gürsevil Turan (METU, PHYS) _____

I hereby declare that all information in this document has been obtained and presented in accordance with academic rules and ethical conduct. I also declare that, as required by these rules and conduct, I have fully cited and referenced all material and results that are not original to this work.

Murat Tamer Ataol

ABSTRACT

MULTIDIMENSIONAL QUANTUM TUNNELLING FORMULATION OF OXYGEN-16 AND URANIUM-238 REACTION

Ataol, Murat Tamer

Ms., Department of Physics

Supervisor: Prof. Dr. Osman Yılmaz

Co-Supervisor: Prof.Dr. Şakir Ayık

June 2004, 51 pages.

Multidimensional quantum tunnelling is an important tool that is used in many areas of physics and chemistry. Sub-barrier fusion reactions of heavy-ions are governed by quantum tunnelling. However, the complexity of the structures of heavy-ions does not allow us to use simple one-dimensional tunnelling equations to find the tunnelling probabilities. Instead of this one should consider all the degrees of freedom which affect the phenomenon and accordingly the intrinsic structure or the deformation of the nuclei must be taken into account in the modelling of heavy-ion fusion. These extra degrees of freedom result in a coupling potential term in the Schrodinger equation of the fusing system. In this thesis $^{16}O +^{238} U$ system is considered. Only the rotational deformation of Uranium is assumed and the coupling potential term is calculated for this system by using two different potential types, namely the Woods-Saxon potential and the double folding potential. Using this term in the Schrodinger equation fusion probability and theoretical cross section are calculated. A discussion that addresses the necessity of multidimensional formulation is given. Besides this point the effects of the choice of the potential type are shown.

Keywords: Multidimensional quantum tunnelling, dissipative quantum tunnelling, fusion, heavy-ion fusion, superheavy elements

ÖZ

OKSİJEN-16 URANYUM-238 REAKSİYONUNUN ÇOK BOYUTLU KUANTUM TÜNEL OLAYI FORMÜLASYONU

Ataol, Murat Tamer
Yüksek Lisans , Fizik Bölümü
Tez Yöneticisi: Prof. Dr. Osman Yılmaz
Ortak Tez Yöneticisi: Prof.Dr. Şakir Ayık

Haziran 2004, 51 sayfa.

Çok boyutlu kuantum tünel olayı fizik ve kimyanın birçok dalında kullanılan önemli bir yöntemdir. Ağır iyonların engel altı füzyon reaksiyonları kuantum tünel olayı ile açıklanır. Ancak ağır iyonların yapılarının karmaşıklığı tünel olasılıklarının bulunmasında basit bir boyutlu tünel denkleminin kullanılmasına izin vermez. Bunun yerine olayları etkileyen bütün etkenler düşünülmeli ve dolayısıyla çekirdeğin iç yapısı ya da çekirdeklerin deformasyonları ağır iyon füzyonunun modellemesinde hesaba katılmalıdır. Bu fazladan etkenler füzyon sistemi için yazılan Schrodinger denkleminde bir eşleme potansiyeli teriminin ortaya çıkmasına neden olurlar. Bu tezde ^{16}O+^{238}U sistemi düşünüldü. Uranyum çekirdeğinin sadece dönme deformasyonu olduğu varsayıldı ve bu sistem için iki değişik potansiyel tipi olan Woods-Saxon potansiyeli ve çift katlamalı potansiyel kullanılarak eşleme terimi hesaplandı. Bu eşleme terimi Schrodinger denkleminde yerine konularak sistem için füzyon olasılığı ve teorik tesir kesiti hesplandı. Çok boyutlu formulasyonun gerekliliği tartışıldı. Ayrıca potansiyel tipi seçiminin etkileri de gösterildi.

Anahtar Sözcükler: çok boyutlu kuantum tünel olayı, dağıtıcı etkili kuantum tünel olayı, füzyon, ağır iyon füzyonu, cok ağır elementler

To My Family...

ACKNOWLEDGMENTS

I thank to my supervisor Prof. Dr. Osman Yılmaz, co-supervisor Prof. Dr. Şakir Ayık, and Prof. Dr. Ahmet Gökalp for their guidance, invaluable comments and patiently supporting me. I am also grateful to my colleague Vedat Tanrıverdi for all his help and contributions. Thank you all sincerely.

I am grateful to Professor Noboru Takigawa who taught me the subject. I thank Takayuki Takehi for his gently and patiently answering all my questions about the subject. I am also grateful to all members of the Nuclear Physics group at Tohoku University, Japan, for their hospitality and kindness.

My special thanks go to my family. Without continuous support and help of my family I couldn't have finished neither this work nor my all other studies. Thank you mummy, dad and sister...

TABLE OF CONTENTS

LIST OF FIGURES

CHAPTER 1

INTRODUCTON

1.1 The Problem

One of the most popular subjects of nuclear physics is fusion. Since its discovery as an energy producing reaction in the stars, it has been thought that if it is understood fully, fusion reaction can be used to supply all energy needs of the world. However, recently it has been realized that, apart from energy considerations, investigating the fusion reactions of different nuclei may be helpful to have new insights into the reaction dynamics and the structure of nuclear matter [1]. Also it has been seen that heavy ion fusion reactions give rise to the formation of super heavy elements, which is another popular and interesting subject of nuclear physics. Because of these reasons, there is much effort to understand the physics of fusion wholly [2].

In the past, nuclear fusion reactions below the Coulomb barrier used to be described by a basic tunnelling model in which one assumes a one dimensional, real potential barrier formed by the repulsive Coulomb and attractive strong interactions. The shape, location and height of these potential barriers were represented by a few parameters which were varied to fit the required cross sections. These potentials are studied and discussed extensively in [3]. In the eighties the results

of the experiments showed that for intermediate mass systems, whose definition will be given in the following sections, the fusion cross sections are much larger than those expected from the simple one dimensional potential model [4, 5]. The inadequacy of this one dimensional potential model was explicitly demonstrated in [6].

With the invent of the advanced experimental techniques and measurement methods in nuclear physics [7, 8], now it is possible to study the effects that enhance the sub-barrier fusion cross sections. Although it is not easy to find out the physical reasons that cause the cross section enhancement, it is known today that any coupling between the relative motions of the nuclei and the intrinsic degrees of freedom of the projectile and target enhances the fusion cross section at sub-barrier energies [9, 10, 11, 12, 13]. This implies that during the tunnelling the nuclei do not behave like point objects but they may be excited, that is ground state is coupled to excited states. In the literature this is called dissipative tunnelling or multidimensional tunnelling. It should be mentioned, however, that every coupling between relative motion and the intrinsic motion do not enhance the cross section at the same level. For example coupling of the single-particle excited states to the relative motion is small and consequently they do not change the cross section appreciably. On the other hand, coupling of the collective states of deformed nuclei, especially rotational and vibrational states, enhances fusion cross section notably [25].

Heavy ion fusion at sub-barrier energies is one example of the multidimensional quantum tunnelling. The standard way to study the relative coupling in fusion

reactions below the Coulomb barrier is the coupled channels formalism [2, 14, 15]. In this formalism, the Hamiltonian of the projectile-target system is rewritten by including both the intrinsic Hamiltonian of the nuclei and the coupling potential between the relative and intrinsic degrees of freedom. So, apart from the bare potential there is a coupling potential in the reaction. The coupling potential depends on the type of the intrinsic excitation of the nuclei and initial angular momentum of the system. More clearly, the physical explanation of the use of coupled channels equations in sub-barrier fusion reactions is that, the nucleus starts tunnelling in its ground state; however, during the passage of the nucleus through the potential barrier, i.e. during it is tunnelling through the barrier, its internal structure may not stay in the ground state. Instead, it may be excited to upper states during the process and there is a certain difference in the tunnelling probabilities of the ground state nucleus and an excited nucleus. Using coupled channels equations, we can figure out how these intrinsic excitations affect the tunnelling probability quantitatively.

In this thesis, the multidimensional quantum tunnelling model will be used to explain the experimental data of heavy ion fusion reactions. A particular system, which is ^{16}O+^{238}U, will be chosen and as described above, coupled channels equations for this system will be solved numerically to obtain the tunnelling probability and the fusion cross section at sub-barrier energies. In the formulation of the coupled channels equations the nuclear potential will be obtained in two different ways, by using Woods-Saxon potential and double folding potential, and the results obtained from these two cases will be compared. It is known that only

the coupling to the collectively excited (relatively low energy) states of nuclei make an important contribution to the cross section. Since ^{16}O is a spherical nucleus, only the deformation of ^{238}U and consequently the collectively excited states of ^{238}U will be considered.

1.2 Multidimensional Quantum Tunnelling

According to classical theories, particles can not enter regions of potential whose energy is greater than the kinetic energy of the particles. One of the most interesting results of quantum mechanics is that, opposite to the classical theories, particles may pass through high potential barriers to transfer from one side of the barrier to the other. This process is called tunnelling. By tunnelling process it is possible for the trapped particles to go out of the potential well without having enough energy to overcome the barrier. One common example of this is the α-particle emission from heavy nuclei. Inside such a nucleus although an α-particle does not have enough kinetic energy to overcome the strong potential, it nevertheless tunnels through it and goes out of the nucleus. The opposite of this situation is also possible. Particles or even small composite systems may tunnel through a potential barrier to enter a potential well. An example of this case is the fusion, which will be discussed in this thesis. Nuclei, with energies much below the barrier may enter inside this barrier and a compound nucleus is formed.

Quantum tunnelling through one, two or three-dimensional potentials may be considered and the tunnelling probabilities for such cases may be calculated by

straightforward techniques. However, generally the tunnelling particle is taken as a point particle for these calculations. If a particle tunnelling through a barrier interacts with its environment then its behavior changes and its intrinsic degrees of freedom are included in the description of the process. Accordingly, the tunnelling takes place in multidimensional space. The first attempt to address the problem of multidimensional quantum tunnelling was that of Kapur and Pierls in 1937 [16]. Later, their theory has been developed by a number of physicist [17, 18, 19]. If the tunnelling system is a large system in which the tunnelling variable couples to a large number of degrees of freedom, then the coupling generally has a dissipative character. Consequently, multidimensional quantum tunnelling is also called dissipative tunnelling [20]. Multidimensional quantum tunnelling plays an important role in many branches of physics and chemistry. Nucleation in ^{3}He-^{4}He systems [21], diffusion of heavy particles in metals [22], the inflation in the early universe [23] are some examples. In some of these systems the tunnelling probability is reduced by the coupling whereas it is enhanced in others. Heavy ion fusion reactions are examples of the latter case.

1.3 Fusion

Fusion is defined as a reaction where two separate nuclei combine to form one nucleus. When two nuclei approach each other sufficiently their interaction is predominantly determined by Coulomb and strong forces. By changing the reference frame from CM frame to the laboratory frame, we can speak in terms of projectile and target nucleus. Since Coulomb force has longer range than nuclear

force, approaching nuclei will first see a Coulomb barrier of the target nucleus before fusion. If this barrier is overcome by the projectile nucleus then because of the strong pull of the nuclear force, two nuclei will form a composite system. This way one heavy nucleus is formed by two small nuclei. A commonly given example of this phenomenon is the formation of ^{2}He nucleus from two separate ^{1}H nuclei in the sun.

$$
\begin{aligned}
{}^1_1H + {}^1_1H &\longrightarrow {}^2_1H + {}^0_{-1}e + \nu \\
{}^2_1H + {}^2_1H &\longrightarrow {}^3_2He + \gamma \\
{}^2_1H + {}^3_2He &\longrightarrow {}^4_2He + {}^0_1e^+ + \nu.
\end{aligned}
$$

The class of fusion reactions, in which nuclei with $A > 4$ are involved, is named as heavy ion fusion. If the sum of the charge of the target and the projectile nuclei is larger than around 12 and the charge product is less than around 1800 the system is said to be an intermediate-mass system. For such systems if the incident energy is not so high, the fusion is governed by the quantum tunnelling over the Coulomb barrier which is created by the Coulomb repulsion of the positive charges of nuclei and the attraction of the strong force of nuclei at much closer distances.

1.4 Heavy Ion Collisions

All nuclei with $A > 4$ are regarded as heavy ions. Because of their relatively high mass if a heavy ion is used as a projectile it will have a very short de Broglie wavelength when compared to the nuclear size. This allows us to describe heavy ion collisions in terms of classical trajectories.

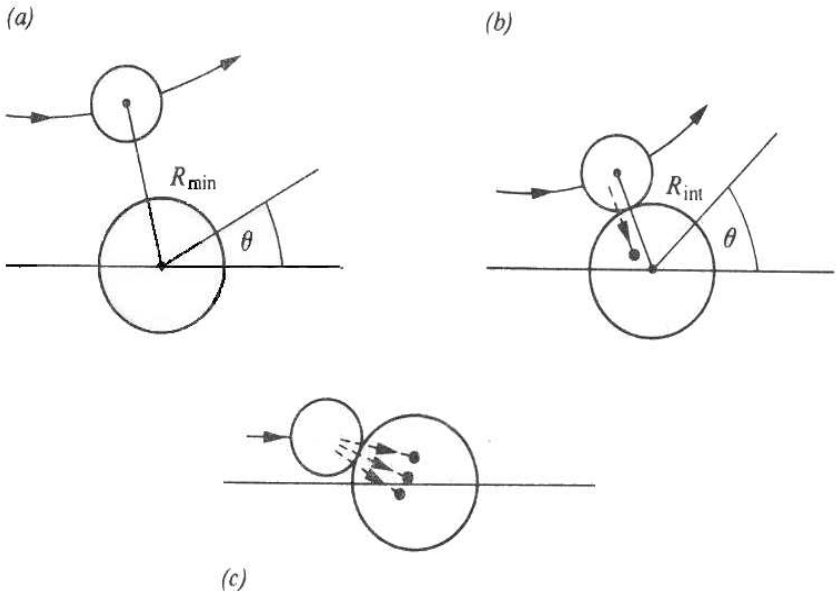

Figure 1.1: Heavy Ion Collisions for different impact parameters. a) Distant collision, b) Grazing trajectory, c) Formation of compound state.

In Fig. 1.1 three general types of collisions between heavy ions are shown. Here the most general potential between the nuclei is given by

$$V = V_n + \frac{Z_P Z_T e^2}{4\pi\epsilon_0} + \frac{L(L+1)\hbar^2}{2\mu r^2}. \tag{1.1}$$

In this equation the last term is the so-called centrifugal potential caused by the total angular momentum of the system which is determined by the initial impact parameter. For the three cases in Fig. 1.1 the following explanations can be given:

1. Distant Collision: This case is shown in Fig. 1.1.a. Here the initial impact parameter is so large that the nuclear force is never felt by the nuclei. So, only Rutherford scattering takes place for energies below the Coulomb barrier.

2. Grazing Trajectory: This trajectory is shown in Fig. 1.1.b. For grazing

angle scattering, if the energy is sufficiently high the nuclear surfaces come so close to each other and the strong attraction, besides the Coulomb repulsion is felt by the nuclei or at least by the surface nucleons. If the incident energy is not above the barrier then some particles, especially neutrons may tunnel through the potential barrier and particle transfer between the nuclei occurs.

3. Very small impact parameters: This is the case which causes the fusion reaction that will be investigated in this thesis and it is shown in Fig. 1.1.c. If incident energy is higher than the Coulomb barrier, most probably compound nucleus formation or fusion occurs. If the energy is below the Coulomb barrier, still fusion or compound nucleus formation may occur but with a smaller probability. Other effects such as intrinsic excitation of the nuclei or particle transfer etc... accompany the fusion. In the following chapters the cross section of the fusion reaction for sub-barrier energies will be calculated by assuming that both the fusion and the intrinsic excitation of the nuclei are involved in the collision.

1.5 Fusion Cross Section

In nuclear and particle physics, because of the small size of the systems, we investigate the structure and dynamics by high energy collisions. To be able to test experimentally, all theoretical result must be expressed in terms of the physical quantities that can be observed experimentally. For the case of collisions

the best observable to interpret is the cross section. It is a function of energy and each reaction has its own cross section. Accordingly, to be able to compare the theoretical and the experimental results, the fusion cross section of intermediate-mass systems will be calculated in this work.

Theoretically the fusion cross section can be calculated by using the method of partial waves. If we denote the fusion probability of a partial wave, with angular momentum L and energy E, by $P_L(E)$ then for the fusion cross section we find

$$\sigma_f(E) = \frac{\pi}{k^2} \sum_L (2L+1) P_L(E). \tag{1.2}$$

Experimentally, when the projectile overcomes the Coulomb barrier of the target and reaches the region of strong attractive force, the nuclei form a composite system. Since the total angular momentum must be conserved before and after the collision, this composite system has a very high angular momentum, which is equal to the sum of the initial orbital and spin angular momenta of the system. Also this system happens to be highly energetic. So it cannot live long and decays into products by giving its excess energy to the decay products as kinetic energy. The lifetime of the compound nucleus is roughly between 10^{-16} s and 10^{-19} s. The compound nucleus decays in two ways, either (I) by emitting light particles such as neutrons, protons or α-particles or (II) by fission. In the former case the compound system ends up with an evaporation residue and then further cools down by emitting high energy rays. In the latter case the excess energy and the angular momentum is released by splitting into two or more fragments and these fragments sometimes are accompanied by light particles. The probability

of occurrence of these processes depends on the incident energy in addition to the initial total angular momentum. The total cross section of the fusion reaction is given by the sum of the fusion-fission and fusion-evaporation cross sections [24]. So, we can compare this experimental and the theoretical cross sections, which are given as above, to the theoretical and experimental results.

1.6 Superheavy Elements

As in atomic physics, there are magic numbers in nuclear physics. They are

$$2, 8, 20, 28, 50, 82, 126, 184\ldots.$$

If the number of protons or neutrons in a nucleus is equal to one of the magic numbers then this nucleus is more stable than others. This fact is explained by the shell model of atomic nuclei. These numbers correspond to the shell closures. However, if we consider the discovered elements up to now, there is an upper limit of Z, and consequently A, for the stable nuclei. On the other hand there are magic numbers greater than the known limits. There the question arises. Are there stable elements with higher Z and A? For example 126-proton and 184-neutron nucleus would be stable according to the shell model, whereas it has not been observed experimentally yet. The elements which have high proton number and which are not naturally occurring are called superheavy elements. Some early theoretical considerations and today's nuclear synthesis experiments suggest that there is an island of stability, which is located around 114 for p number and around 184 for n number in the p-n graph as shown in Fig. 2.2.

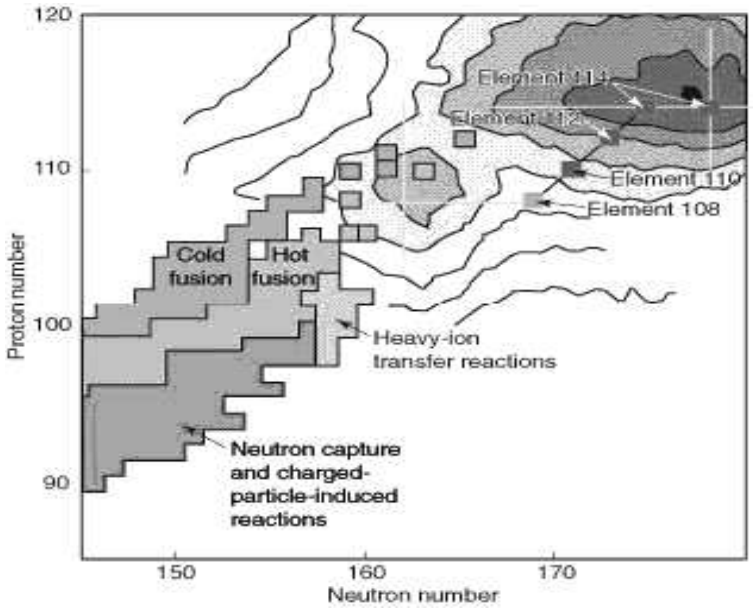

Figure 1.2: The island of stability of superheavy elements. Taken from [26].

Recently, superheavy elements in this region, with $A = 112$, $A = 114$, and $A = 116$ have been observed as the product of heavy ion fusion reactions [26]. The creation of new superheavy elements would be helpful in understanding the nuclear structure and the structure of the matter in the early universe. So, this is one of the many motivations for studying the heavy ion fusion reactions.

CHAPTER 2

FORMALISM

2.1 Fusion in the One Dimensional Tunnelling Model

The most basic formulation of the heavy ion fusion reactions is given by using a one dimensional quantum tunnelling model. The potential between the projectile and the target nuclei is given by

$$V_L(r) = V_N(r) + V_C(r) + \frac{L(L+1)\hbar^2}{2\mu r^2}. \tag{2.1}$$

The $L = 0$ barrier is referred to as the Coulomb barrier. The barrier shapes for different L values are shown in Fig. 2.1.

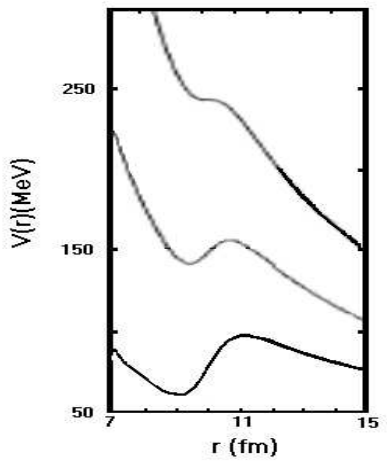

Figure 2.1: One dimensional potential barrier for ^{64}Ni+^{64}Ni for different values of L. The lowest barrier is for $L = 0$. The middle and the highest barriers are for $L = 100$ and $L = 150$ respectively. (Taken from [2])

The transmission probabilities through this barrier can be calculated by using WKB approximation [27, 28]. In this calculation the potential barrier for $L = 0$ is approximated by a parabola

$$V_0 = V_{B0} - \frac{1}{2}\mu^2\Omega^2(r - r_0)^2 \tag{2.2}$$

where V_{B0} is the height and $\hbar\Omega$ is the measure of the curvature of the barrier, as shown in Fig. 2.2.

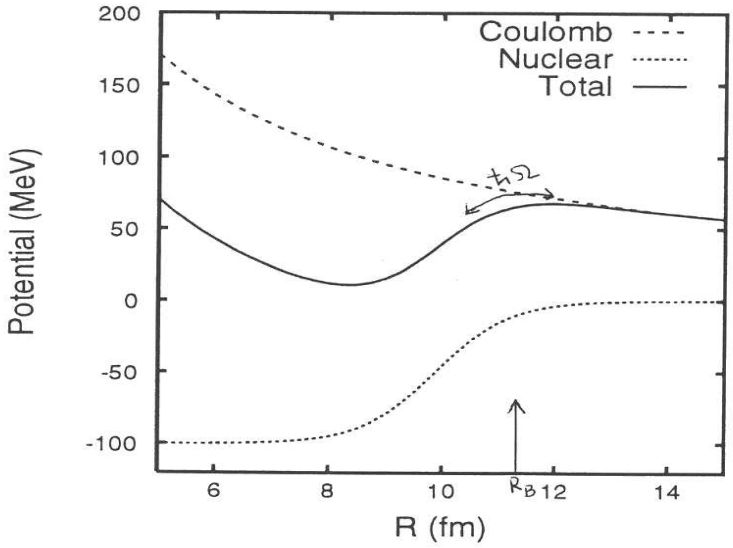

Figure 2.2: The interaction potential for heavy-ions and the curvature, $\hbar\Omega$, of the barrier.

With this approximation the $L = 0$ wave transmission probability can be calculated to be [29]

$$P_0(E) = \frac{1}{1 + \exp\left[-\frac{2\pi}{\hbar\Omega}(E - V_{B0})\right]}. \tag{2.3}$$

To find the tunnelling probability for $L > 0$ we simply shift the energy in $P_0(E)$ by assuming that the barrier position and the curvature, $\hbar\Omega$, do not depend on

angular momentum. Under these assumptions we have

$$P_L(E) = P_0 \left(E - \frac{L(L+1)}{2\mu r^2} \right). \tag{2.4}$$

Using these transmission probabilities one can obtain the Wong formula for the fusion cross section in this one dimensional model [9]

$$\sigma(E) = \frac{\hbar\Omega r_0^2}{2E} \ln \left\{ 1 + \exp\left[\frac{2\pi}{\hbar\Omega}(E - V_{B0}) \right] \right\}. \tag{2.5}$$

For energies below the barrier, i.e. $E \ll V_{B0}$, the cross section can be approximated by

$$\sigma(E) \approx \frac{\hbar\Omega r_0^2}{2E} \exp\left\{ \frac{2\pi}{\hbar\Omega}(E - V_{B0}) \right\}. \tag{2.6}$$

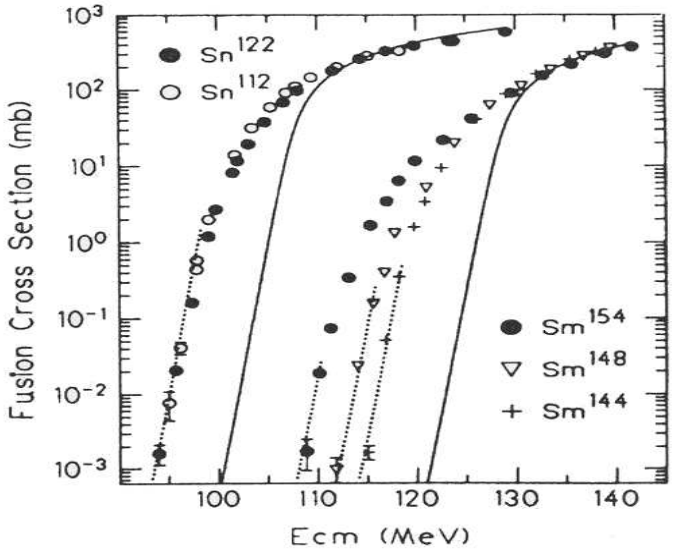

Figure 2.3: Cross sections for several intermediate-mass systems. Experimental and theoretical results obtained from Wong formula are plotted for comparison. Taken from [12].

The theoretical cross sections obtained from the Wong formula, by fitting R_B, $\hbar\Omega$ and V_{B0} to reproduce the data at high energies, are given in Fig. 2.3 for

$^{40}Ar +^{112} Sn$, $^{40}Ar +^{122} Sn$, $^{40}Ar +^{144} Sm$, $^{40}Ar +^{148} Sm$, $^{40}Ar +^{154} Sm$ reactions. The Coulomb barriers for these collisions are 110 MeV for collisions including Sn target, 130 MeV for collisions including Sm target. It is seen from the graphs that, for sub-barrier energies, the cross sections obtained from the one dimensional model are substantially smaller than the experimental ones.

This comparison clearly shows the importance of the intrinsic excitations of the fusing nuclei. It is also seen from the figure that for different isotopes of the same element the enhancement of the cross section changes. This is another proof that the enhancement is because of the intrinsic structure.

So, from the beginning of the problem this intrinsic effect must be taken into account. In the following sections, the formulation of the problem will be performed to see the effects of the intrinsic excitations to the fusion cross section at sub-barrier energies.

2.2 Fusion in the Multidimensional Tunnelling Model

As it is noted before, a one dimensional approach is inadequate for the theory of fusion. It does not reproduce the experimental data well, especially for energies below the barrier. In this chapter, we will follow a different route to formulate the same problem. Here, as opposed to the one dimensional tunnelling case, the tunnelling nucleus will be assumed to have an intrinsic structure. We will consider a reaction between ^{16}O and ^{238}U with incident energy from 70 MeV to 100 MeV. So, we need to elaborate how ^{16}O and ^{238}U behave in collisions at these energies.

For the energy range specified above, ^{16}O nucleus behaves like a point particle.

This is easy to understand if we remember that ^{16}O is a closed shell nucleus with 8 protons and 8 neutrons. This type of nucleus can generally have single particle excited states, which is similar to the excited states of an atom. One proton or neutron is excited to an upper energy level. These excitations are not likely to be observed for the energies considered here, because they have high energies. Even if they are observed, as it is explained before, the coupling of these states to the relative motion is small and consequently its effect to the cross section is negligible. The other possibility of excitation is the collective excitation of the ^{16}O nucleus. However, being a closed shell nucleus, it does not have collective excited states. Therefore, for the collision considered here ^{16}O can be assumed to be a point particle. It enters the collision as a spherical nucleus and leaves the collision as a spherical one, without changing its internal structure during the process.

For ^{238}U the situation is quite different than ^{16}O. ^{238}U nucleus has 92 protons and 146 neutrons. This shows that nucleus is far from being a spherical nucleus according to the shell model, which says that, the closest magic numbers to these neutron and proton numbers are 82 and 126 respectively. Therefore, ^{238}U have 10 protons more over its closed proton shell and 20 neutrons over its closed neutron shell. This excess of nucleons in ^{238}U makes them behave collectively besides their single particle motions. That is, the collective states of the ^{238}U nucleus couple to the relative motion and create the coupled channels in the fusion reaction. Accordingly, in the tunnelling region ^{238}U nucleus changes its internal structure. That is, while tunnelling over the Coulomb barrier, ^{238}U nucleus is not static.

Extensive studies on heavy ion fusion reactions showed that this is an important factor which affects the tunnelling probability in the fusion reaction. This factor is investigated for a variety of fusion reactions, such as $^{16}O + ^{144}Sm$, $^{40}Ca + ^{124}Sn$ and it is now well understood that the formulation of the fusion reaction by considering the tunnelling of an excited nucleus gives results that is in good agreement with the experimental data [30].

^{238}U nucleus may have rotational and vibrational collective excitations. In principle it is possible to include the coupling of all of these states to the relative motion but this would be a long and complicated problem. Instead one can take a certain set of collective states to investigate their effect to the fusion cross section and then combine the results if necessary. Consequently, in this work rotational states of ^{238}U with $K = 0$, i.e. pure rotational excitation only, will be considered. As for these states, ^{238}U nucleus possesses a symmetry axis, which we label as the z-axis in the body fixed coordinate system. In this coordinate system the shape of the nucleus is invariant to the rotations about the z-axis. So the nucleus cannot have angular momentum components along this direction. The situation for ^{238}U is explained in detail in Appendix A. Accordingly the excited states of ^{238}U have $I = 0, 2, 4, 6, 8 \ldots$ They are shown schematically in Fig. 2.4

For the theoretical calculation of the tunnelling probabilities we start by writing the Schrodinger equation for this system.

$$H\Psi = E\Psi. \tag{2.7}$$

Here H is the Hamiltonian of the colliding $^{16}O + ^{238}U$ system. In the simple

one dimensional calculations H is given by

$$H = -\frac{\hbar^2}{2\mu}\nabla^2 + V_0(r) \tag{2.8}$$

where the first term represents the kinetic energy and $V_0(r)$ is the Coulomb barrier. In the multidimensional formulation, we replace this Hamiltonian by

$$H = -\frac{\hbar^2}{2\mu}\nabla^2 + V_0(r) + H_0(\xi) + V^{coup}(\vec{r},\xi) \tag{2.9}$$

in which the first two terms represent the same things as in Eq. 2.8 and the third and fourth terms represent the intrinsic structure of ^{238}U and the coupling of the relative motion to the excited states of ^{238}U nucleus, respectively. As it is shown in Eq. 2.9, H_0 is a function of the intrinsic coordinates ξ and satisfies the relationship

$$H_0|nIm_I\rangle = \varepsilon_{nI}|nIm_I\rangle. \tag{2.10}$$

$V^{coup}(\vec{r},\xi)$ depends on both the relative and intrinsic coordinates. Using the Hamiltonian given in Eq. 2.9, our Schrodinger equation for the multidimensional formulation becomes

$$H\Psi = \left(-\frac{\hbar^2}{2\mu}\nabla^2 + V_0(r) + H_0(\xi) + V^{coup}(\vec{r},\xi)\right)\Psi = E\Psi. \tag{2.11}$$

In this equation Ψ depends on the coordinates r and ξ. That is, Ψ is obtained by the combination of the relative and intrinsic wave functions, $|Lm_L\rangle$ and $|nIm_I\rangle$ respectively. To construct Ψ we start with the inner product of the relative and intrinsic wave functions

$$|Lm_L\rangle \otimes |nIm_I\rangle = |nLIm_Lm_I\rangle. \tag{2.12}$$

However, in this problem we are dealing with the total angular momentum. Therefore by using the Clebsh-Gordon coefficients we switch to the basis in which total angular momentum is included

$$|nLIJm_J\rangle = \sum_{nm_Lm_I} |nLIm_Lm_I\rangle\langle nLIm_Lm_I|nLIJM\rangle \tag{2.13}$$

and this way Ψ becomes

$$\Psi = \sum_{nLI} \frac{\phi^J_{nLI}}{r}|nLIJM\rangle. \tag{2.14}$$

In Eq. 2.14, ϕ^J_{nLI} stands for the radial part of the $^{16}O +^{238} U$ system. It does not include angular components. When we solve the Schrodinger equation, Eq. 2.11, and obtain ϕ^J_{nLI}, then ϕ^J_{nLI} contains all the information we need to find the tunnelling probability. To solve the Schrodinger equation we insert Eq. 2.14 into Eq. 2.11. The Schrodinger equation then becomes

$$\sum_{n'L'I'} \left\{ -\frac{\hbar^2}{2\mu}\nabla^2 + V_0(r) + H_0(\xi) + V^{coup}(\vec{r},\xi) \right\} \frac{\phi^J_{n'L'I'}}{r}|nLIJM\rangle = E\Psi \tag{2.15}$$

in which the kinetic energy operator can be separated into radial and angular parts as

$$-\frac{\hbar^2}{2\mu}\nabla^2 = -\frac{\hbar^2}{2\mu}\frac{1}{r^2}\frac{\partial}{\partial r}(r^2\frac{\partial}{\partial r}) + \frac{L^2}{2\mu r^2} \tag{2.16}$$

where

$$L^2|nLIJM\rangle = L(L+1)\hbar^2|nLIJM\rangle. \tag{2.17}$$

By this separation and using the Eq. 2.10, Eq. 2.15 is reduced to

$$\left(-\frac{\hbar^2}{2\mu}\frac{d}{dr^2} + \frac{L(L+1)\hbar^2}{2\mu r^2} + V_0(r) + \varepsilon_{nI} - E\right)\phi^J_{nLI} + \sum_{n'L'I'} \langle nLIJM|V^{coup}|n'L'I'J'M'\rangle\phi^J_{n'L'I'} = 0. \tag{2.18}$$

We need to solve this equation to find the ϕ^J_{nLI} functions. Eq. 2.10 denotes a set of second order differential equations of the radial variable r. In this equation E is the bombarding energy of the incident particles, L stands for the radial angular momentum of the $^{16}O + ^{238}U$ system, and ε_{nI} is the energy eigenvalue of the intrinsic excited states of the ^{238}U nucleus. This eigenvalue depends on the excitation type. In this work the rotational excited states with $K = 0$ will be considered only. Accordingly the rotational Hamiltonian of ^{238}U nucleus is given by

$$H_R = \frac{I^2}{2M} \tag{2.19}$$

from which ε_{nI} can be found by using the eigenvalue equation for the intrinsic rotation. This eigenvalue equation reads

$$H_R|nIm_I\rangle = \frac{I^2}{2M}|nIm_I\rangle = \varepsilon_{nI}|nIm_I\rangle = \frac{I(I+1)\hbar^2}{2M}|nIm_I\rangle \tag{2.20}$$

where I is the intrinsic angular momentum operator and M is the moment of inertia about the axis of rotation. So value of ε_{nI} can be found from this expression by using the experimentally measured values of moment of inertia, M, of the nucleus ^{238}U.

2.2.1 Iso-centrifugal Approximation

The Schrodinger equation for $^{16}O + ^{238}U$ system, Eq. 2.18, is a set of differential equations to be solved simultaneously. If the number of excited states of the target nucleus that couples to the relative motion gets larger, then the number of differential equations to be solved simultaneously becomes very large. For

example, for rotational excitation, if coupled states are only the ground and first excited states then we have four second order differential equations, if coupled states are up to the second excited state then we have nine second order differential equations, which is because of the degeneracy of the states as shown in the Fig. 2.4. As the coupled states increase, the equation number increases and Eq. 2.18 becomes very hard to solve. To be able to solve Eq. 2.18, the number of coupled channels must be decreased by a fair approximation. Iso-centrifugal approximation serves for this purpose.

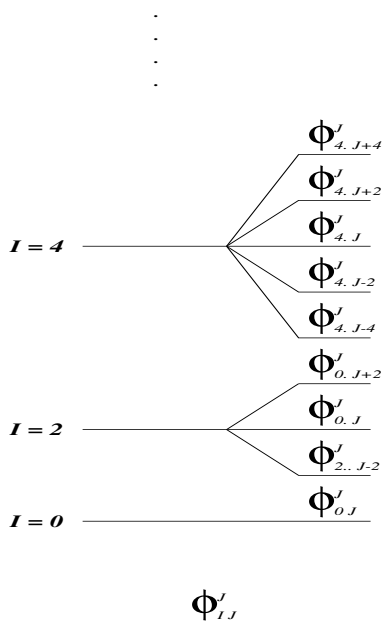

Figure 2.4: Excited rotational states of ^{238}U nucleus with wave functions.

Without any approximation, the ground state, the excited states and the corresponding radial wave functions are shown in Fig. 2.4. In principle there may be coupling between all those states in a fusion reaction. In the iso-centrifugal approximation we transform the system to the body-fixed coordinates and the

centrifugal potential energy in Eq. 2.18, $\frac{L(L+1)}{2\mu r^2}$, is replaced by $\frac{J(J+1)}{2\mu r^2}$. In the body-fixed coordinate system one reduces the number of coupling between intrinsic states by obtaining new states which are the linear combination of the original states. A unitary transformation of the form

$$\phi_I^{'J} = \sum_L U_{\alpha,L}^{(I,J)} \phi_{nLI}^J \tag{2.21}$$

transforms the original physical wave functions ϕ_{nLI}^J to $\phi_I^{'J}$ which are mathematical representations of the same sets of excited states. These states are shown schematically in Fig. 2.5. One can prove that [35], only the wave function ob-

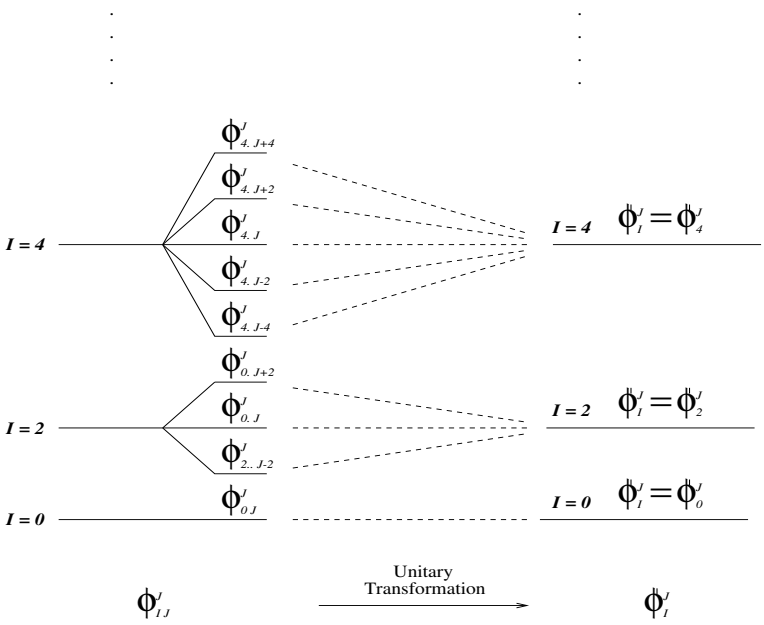

Figure 2.5: Transformed rotational states of ^{238}U nucleus with wave functions.

tained by setting $\alpha = 1$ among all $\phi_I^{'J}$ appears in the coupled channels equations if $U_{\alpha,L}^{(I,J)}$ is chosen such that

$$U_{\alpha=1,L}^{(I,J)} = i^{-I-L}\sqrt{\frac{2L+1}{2J+1}}\langle LI00|J0\rangle. \tag{2.22}$$

So with the new set of wave functions, V^{coup} matrix is reduced in dimension

and it is diagonalized. In the transformed form, Eq. 2.18 can be rewritten as

$$\left(-\frac{\hbar^2}{2\mu}\frac{d^2}{dr^2}+\frac{J(J+1)\hbar^2}{2\mu r^2}+V_0(r)+\varepsilon_{nI}-E\right)\phi_I^{\prime J}+V^{\prime coup}\phi_I^{\prime J}=0 \qquad (2.23)$$

where $V^{\prime coup}$ is the reduced and diagonalized form of V^{coup} and can be obtained by

$$V^{\prime coup}=U^{-1}V^{coup}U. \qquad (2.24)$$

Iso-centrifugal approximation is first introduced in chemistry with the name centrifugal sudden approximation [31, 32]. With this approximation the angular dependence of the coupling operator disappears and the number of coupled states are reduced [33]. It has been shown that iso-centrifugal approximation results in negligible errors in the heavy-ion fusion cross section calculations [34].

2.2.2 Form of the Coupling Potential

The most important operator in Eq. 2.23 that must be described is the coupling potential. To determine its form it is better to start with the total potential V which is the sum of the bare potential V_0 and the coupling potential V^{coup}:

$$V=V_0+V^{coup}. \qquad (2.25)$$

Here V_0 and V^{coup} have two parts, the Coulomb part resulting from the charges of both nuclei and the nuclear part resulting from the strong interaction of the nucleons in both nuclei. So, in more detail, V_0 and V^{coup} can be written as

$$\begin{aligned} V=V_0+V^{coup} &= (V_{0C}+V_C^{coup})+(V_{0N}+V_N^{coup}) \\ V^{coup} &= V_C^{coup}+V_N^{coup}. \end{aligned} \qquad (2.26)$$

Consequently, to determine the form of V^{coup} we need to determine first the form of V_C^{coup} and V_N^{coup}.

In this work Eq. 2.23 will be solved and the corresponding $\phi_I^{'J}$ will be obtained for two different forms of V^{coup}. Firstly, the Coulomb part, V_C^{coup}, will be found by using the familiar Coulomb law and the nuclear part, V_N^{coup}, will be calculated by assuming that the nuclear potential has the well known Woods-Saxon shape. By inserting this form of V^{coup} Eq. 2.23 will be solved and the corresponding cross sections will be obtained by using the functions $\phi_I^{'J}$.

The second calculation to obtain the same cross section will also be performed but in this case with a different form of V^{coup}. In this second calculation the Coulomb part and the nuclear part, V_C^{coup} and V_N^{coup} respectively, will be obtained by using the double-folded potential calculations. This second form of V^{coup} will be inserted in Eq. 2.23 and the corresponding cross section will be obtained.

2.2.3 Form of the Coupling Potential by Using Woods-Saxon and Coulomb Potential

Empirical results obtained from nuclear physics experiments show that Woods-Saxon potential is a good representation of the nuclear potential in most cases. Accordingly, the nuclear potential in Eq. 2.23 can be taken in the Woods-Saxon form, which is given as

$$V = \frac{-V_0}{1 + \exp(\frac{r - R_0}{a_0})}. \tag{2.27}$$

The plot of this potential is shown in the Fig. 2.6 along with the harmonic oscillator potential for comparison.

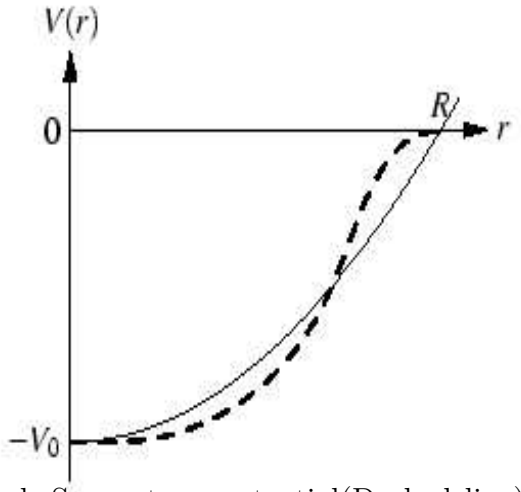

Figure 2.6: Plot of Woods-Saxon type potential(Dashed line). Square well potential (continuous line) is also plotted for comparison.

In a heavy ion collision, R_0 in Eq. 2.27 is taken as the distance between the centers of the colliding nuclei, that is

$$R_0 = R_P + R_T = r_0(A_P^{1/3} + A_T^{1/3}). \tag{2.28}$$

However, in the heavy ion reaction considered in this work, one of the colliding nuclei, namely the target is deformed. So, R_T is not constant and given by

$$R_T(r,\theta,\phi) = R_{T0}\left(1 + \sum_{\lambda\mu} \alpha_{\lambda\mu}(r) Y_{\lambda\mu}(\theta,\phi)\right). \tag{2.29}$$

Now that the form of the potential and the parameters have been determined, the explicit form of V^{coup} can be found. The nuclear potential between the colliding nuclei is written as

$$V_N = \frac{-V_0}{1+\exp\left(\frac{r-R_0-\delta R}{a_0}\right)} = \frac{-V_0}{1+\exp\left(\frac{r-R_0-R_{T0}\sum_{\lambda\mu}\alpha_{\lambda\mu}(r)Y_{\lambda\mu}(\theta\phi)}{a_0}\right)}. \tag{2.30}$$

This potential is valid in any frame. That is, in this form the z-axis is arbitrary. However, by writing the same potential in the body fixed coordinate system a

simpler form of the equation may be obtained. In the body fixed system the z-axis is chosen along the symmetry axis of the nuclei. Since we are considering only the rotationally excited states, K is taken to be zero in the body fixed frame. By the use of Bohr-Mottelson parameters and the $D^{\lambda}_{\mu\mu'}$ functions we have

$$\alpha_{\lambda\mu} = \sum_{\lambda\mu} D^{\lambda}_{\mu\mu'}(\omega) a_{\lambda\mu'} = D^{\lambda}_{\mu 0}\beta_{\lambda} \tag{2.31}$$

and since z-axis is the symmetry axis of the deformed nucleus $Y_{\lambda\mu}$ function can be written as

$$Y_{\lambda\mu}(\theta = 0) = \sqrt{\frac{2\lambda+1}{4\pi}}\delta_{\mu 0}. \tag{2.32}$$

Then the deviation δR becomes

$$\delta R = R_{T0} \sum_{\lambda\mu} D^{\lambda}_{\mu\mu'}(\omega)\beta_{\lambda}\sqrt{\frac{2\lambda+1}{4\pi}}\delta_{\mu 0}. \tag{2.33}$$

In terms of the $D^{\lambda}_{\mu\mu'}$ function $Y_{\lambda\mu}$ is given by

$$Y_{\lambda\mu} = D^{\lambda}_{\mu 0}\sqrt{\frac{2\lambda+1}{4\pi}}. \tag{2.34}$$

Consequently δR can be written as

$$\delta R = R_{T0} \sum_{\lambda} \beta_{\lambda} Y_{\lambda 0}. \tag{2.35}$$

Accordingly nuclear potential has the form

$$V_N = \frac{-V_0}{1 + \exp\left(\frac{r - R_0 - R_{T0}\sum_{\lambda}\beta_{\lambda}Y_{\lambda 0}(\theta)}{a_0}\right)}. \tag{2.36}$$

If we expand this result by the Taylor series expansion about the spherical shape, we have, up to the first order in δR,

$$V_N = \frac{-V_0}{1 + \exp\left(\frac{r-R_0}{a_0}\right)} - \frac{R_{T0}V_0 \exp\left(\frac{r-R_0}{a_0}\right)}{a_0\{\exp\left(\frac{r-R_0}{a_0}\right)\}^2} \sum_{\lambda} \beta_{\lambda} Y_{\lambda 0} \tag{2.37}$$

$$V_N = V_{N0} + V_N^{coup} = V_{N0} + \sum_{\lambda_{even}} f^N(r)\beta_\lambda Y_{\lambda 0} \tag{2.38}$$

where $f^N(r)$ is given by

$$f^N(r) = -\frac{R_{T0}V_0 \exp{(\frac{r-R_0}{a_0})}}{a_0\{\exp{(\frac{r-R_0}{a_0})}\}^2}. \tag{2.39}$$

The parameters V_0, a_0 and R_{T0} for $^{16}O +^{238} U$ are given in Appendix D.

For the Coulomb interaction we start by assuming a uniform charge distribution of the form

$$\rho(r) = \begin{cases} \rho_c, & \text{when } r < R_\beta(\Omega) \\ 0, & \text{when } r > R_\beta(\Omega) \end{cases} \tag{2.40}$$

where $\rho_c = \frac{3Z_T e}{4\pi R_{T0}^3}$ for the target nucleus. So, the Coulomb potential is

$$V_C = eZ_P\rho_C \int d\Omega' \int dr' r'^2 \frac{1}{|\vec{r} - \vec{r'}|}. \tag{2.41}$$

Using the expansion

$$\frac{1}{|\vec{r} - \vec{r'}|} = \sum_{lm} \frac{4\pi}{2l+1} \frac{r_<^l}{r_>^{l+1}} Y_{lm}(\Omega')Y_{lm}(\Omega) \tag{2.42}$$

the integral in Eq. 2.41 can be performed with the standard methods as is shown in Appendix B. The result is found to be

$$V_C = \frac{Z_P Z_T e}{r} + \sum_{\lambda_{even}} \frac{3Z_P Z_T e^2}{2\lambda+1} \frac{R_{T0}^\lambda}{r^{\lambda+1}} \beta_\lambda Y_{\lambda 0}(\theta) \tag{2.43}$$

$$V_C = V_{C0} + V_C^{coup} = V_{C0} + \sum_{\lambda_{even}} f_\lambda^C(R)\beta_\lambda Y_{\lambda 0}(\theta) \tag{2.44}$$

where $f_\lambda^C(R)$ is

$$f_\lambda^C(R) = \frac{3Z_P Z_T e^2}{2\lambda+1}\frac{R_{T0}^\lambda}{r^{\lambda+1}}. \tag{2.45}$$

Accordingly the nuclear and Coulomb potentials combined to give the total potential as

$$V = (V_{N0} + V_{C0}) + (V_N^{coup} + V_C^{coup}) = V_0 + \sum_{\lambda_{even}} (f^N(r) + f_\lambda^C(r))\beta_\lambda Y_{\lambda 0}(\theta) \tag{2.46}$$

from which we can obtain the form of V^{coup}

$$V^{coup} = \sum_{\lambda_{even}} f_\lambda(r)\beta_\lambda Y_{\lambda 0}(\theta). \tag{2.47}$$

A comment should be made for the λ being even in the above summations.β_λ and $Y_{\lambda 0}$ are the terms that describe the deformation of the ^{238}U nucleus. In Eq. 2.23 V^{coup} is an operator and so are $Y_{\lambda 0}$ functions. These operators connect the rotational excited states of the nucleus. Since only $K = 0$ states are involved in the calculations in this work, V^{coup} can connect states with I even. Accordingly in the above summations we take λ even.

2.2.4 Form of the Coupling Potential by Using Double Folding Nuclear and Coulomb Potentials

We can find V^{coup} by following a different route than the one followed in the preceding section. In that section Woods-Saxon potential was used to describe the strong interaction between nuclei. However, other mathematical representations of the nuclear potential can be used by adjusting the constants in those representations according to the experimental data obtained from various nuclear

reactions. In this section Yukawa potential will be used for the nuclear part of the V^{coup}. Yukawa potential is written as

$$V_{Yukawa}(r) = V_0 \frac{e^{-\mu r}}{\mu r} \tag{2.48}$$

where μ and V_0 are constants to be determined from experimental data. The electric interaction has a definite form which is given by Coulombs law. So there is no need to look for alternatives for it.

Besides using an alternative form of strong interaction, an alternative method of calculation will be used in this section. A method, known as double folding, can be used to incorporate the spatial distribution of the nuclear mass and charge of the target and the projectile. In this method the mass and charge distributions of the nuclei are determined and the total nuclear and Coulomb potentials are found by summing the contributions coming from the interaction of each infinitesimal volume element of the target and projectile. Interactions between infinitesimal volume elements along with the position vectors of the nuclei are shown in Fig. 2.7.

In double folding model, V is given by

$$V(\vec{r}, \alpha) = \int d^3 r_P d^3 r_T \rho_P(\vec{r}_P) \rho_T(\vec{r}_T) v(\vec{r}_{12} = \vec{r} + \vec{r}_P - \vec{r}_T) \tag{2.49}$$

where $\rho_P(\vec{r}_P)$ and $\rho_P(\vec{r}_T)$ are the mass (charge) distributions of the projectile and target respectively, for nuclear (Coulomb) part of the potential. The potential $v(\vec{r}_{12} = \vec{r}_P - \vec{r}_T)$ in this equation stands for the potential between two infinitesimal elements of the target and projectile. For nuclear interaction it is Yukawa function and for electric interaction it is Coulomb potential.

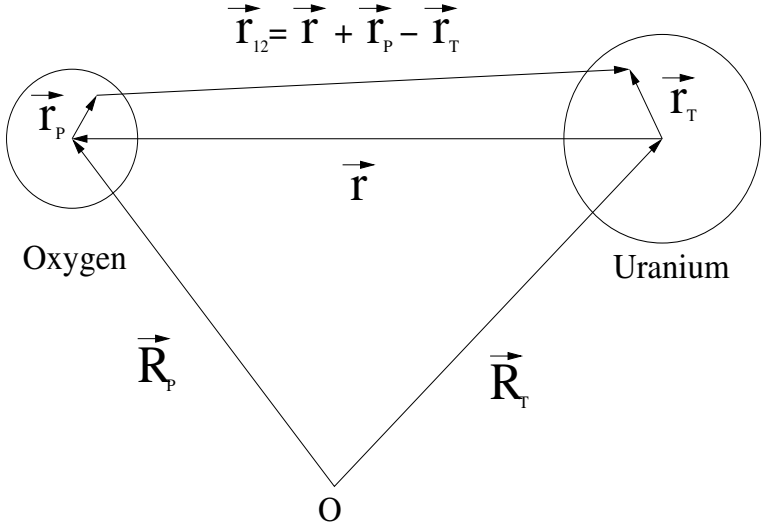

Figure 2.7: Coordinate system and vectors used in the calculation of double folding type potential.

This is a six dimensional integral and it is not easy to evaluate. However, by use of a momentum space method [36], [37], it can be put in a simpler form. If the Fourier transformation of a function $f(x)$ is denoted by $\widetilde{f}(k)$, the following relations hold

$$\begin{aligned} \widetilde{f}(\vec{k}) &= \int d^3x f(\vec{x}) \exp[i\vec{k}\cdot\vec{x}] \\ f(\vec{x}) &= \frac{1}{(2\pi)^3}\int d^3k \widetilde{f}(\vec{k}) \exp[-i\vec{k}\cdot\vec{x}]. \end{aligned} \tag{2.50}$$

So the Fourier transformation of $V(\vec{r},\alpha)$ is given by

$$\begin{aligned} \widetilde{V}(\vec{k},\alpha) &= \int d^3r V(\vec{r},\alpha) \exp[i\vec{k}\cdot\vec{r}] \\ \widetilde{V}(\vec{k},\alpha) &= \int d^3r \exp[i\vec{k}\cdot(\vec{r}_{12}=\vec{r}_P-\vec{r}_T)] v(\vec{r}_{12}=\vec{r}_P-\vec{r}_T) \\ &\quad \times \int d^3r_P \rho_P(\vec{r}_P)\exp[-i\vec{k}\cdot\vec{r}_P]\int d^3r_T\rho_T(\vec{r}_T)\exp[i\vec{k}\cdot\vec{r}_T] \\ \widetilde{V}(\vec{k},\alpha) &= \widetilde{v}(\vec{k})\widetilde{\rho}_P(-\vec{k})\widetilde{\rho}_T(\vec{k}). \end{aligned} \tag{2.51}$$

If we Fourier transform the result one more and use the identity

$$\exp[i\vec{k}\cdot\vec{r}] = \sum_{lm} 4\pi i^l j_l(kr) Y_{lm}(\Omega_k) Y_{lm}(\Omega_r) \tag{2.52}$$

we obtain $V(\vec{r},\alpha)$ as an integral in k space. The result is

$$\begin{aligned} V(\vec{r},\alpha) &= V_0(r) + \sum_{\lambda\mu} \alpha_{\lambda\mu} f_\lambda(r) Y_{\lambda\mu}(\Omega_r) \\ V_0(r) &= 8\rho_0^P \rho_0^T R_{T0}^2 R_P^2 \int_0^\infty dk \frac{j_0(kr) j_1(kR_p) j_1(kR_{T0})}{(1+k^2a_p^2)(1+k^2a_T^2)} \tilde{v}(k) \\ f_\lambda(r) &= 8\rho_0^P \rho_0^T R_{T0}^3 R_P^2 \int_0^\infty dk \frac{j_\lambda(kr) j_1(kR_p) j_\lambda(kR_{T0})}{(1+k^2a_p^2)(1+k^2a_T^2)} \tilde{v}(k). \end{aligned} \tag{2.53}$$

In these equations $\tilde{v}(k)$ is the Fourier transformed form of the potential term. So for nuclear interaction it is written as

$$v(r) = v_0 \frac{a_n e^{-r/a_n}}{r} \overset{four.trans.}{\longrightarrow} \tilde{v}(k) = v_0 \frac{4\pi a_n^3}{(1+k^2a_n^2)} \tag{2.54}$$

and for Coulomb interaction it is given by

$$v(r) = \frac{e^2}{r} \overset{four.trans.}{\longrightarrow} \tilde{v}(k) = \frac{4\pi e^2}{k^2}. \tag{2.55}$$

Solution of the integrals in Eq. 2.53 are given in Appendix C for $\lambda = 0$ and $\lambda = 2$. If we write the equation for V in the body fixed coordinate system of the target then we obtain as in the preceding section

$$V = V_0 + V^{coup} = V_0 + \sum_{\lambda_{even}} f_\lambda(r) \beta_\lambda Y_{\lambda 0}. \tag{2.56}$$

2.2.5 Density Distributions

From experimental data it is known that the charge and mass distributions for ^{16}O and for ^{238}U are approximately the same. So the density distributions will

be taken the same for mass and charge of these nuclei. There are different density distribution functions that can be used to describe nuclei, such as Gaussian function, Yukawa-Step function and Delta function. In this work Yukawa-Step function will be used for both projectile and target. However, as before it will be assumed that ^{16}O is spherical and ^{238}U is deformed.

Nuclear mass and charge distribution of ^{16}O is given by a convolution of the form

$$\rho_P(\vec{r}_P) = \rho_{P0} \int d^3r_P \frac{a_P \exp[-|\vec{r}_P - \vec{r}'|/a_P]}{|\vec{r}_P - \vec{r}'|} \theta[R_P - r'] \tag{2.57}$$

where R_P is the radius of the ^{16}O and the density becomes zero outside this radius. Nuclear mass and charge distribution of ^{238}U are given by a convolution of the same form

$$\rho_T(\vec{r}_T) = \rho_{T0} \int d^3r_T \frac{a_T \exp[-|\vec{r}_T - \vec{r}'|/a_T]}{|\vec{r}_T - \vec{r}'|} \theta[R_T(\alpha) - r']. \tag{2.58}$$

However, in this case the surface of the nucleus is deformed and $R_T(\alpha)$ shows this deformation. It is given by

$$R_T(\alpha) = R_{T0} \left\{ 1 + \sum_{\lambda\mu} \alpha_{\lambda\mu} Y_{\lambda\mu}(\Omega) \right\}. \tag{2.59}$$

2.2.6 Linear Coupling and All Order Coupling

In the above calculations the coupling potentials are given up to first order in deformation parameters β_λ. More accurate results can be obtained by including higher order terms in the Taylor Series expansion. Up to what order should we include in the V^{coup} calculations for a good theoretical result? This is a question that can only be answered by comparing the experimental data with the

calculation. It is now known that Coulomb coupling is well approximated by the linear coupling. So there is no need to include higher order terms in the Coulomb part of the coupling potential.

It is also known from past studies that the higher order couplings are important for the nuclear part of the coupling potential. So higher order terms must be included for nuclear part. This can be done by use of a computer program. For the Woods-Saxon form such a program, namely the CCFULL, is written by K. Hagino, N. Rowley, A.T. Kruppa [38]. That program calculates the Coulomb part of V^{coup} up to second order with respect to β_2 and up to first order with respect to β_4 and the nuclear part of V^{coup} by including all orders with respect to β_λ. This program makes use of a matrix algebra to calculate all orders in the expansion. A description of this algebra can be found in [39].

To find the coupling potential by using the double folding potential we should rewrite the part of the CCFULL program that calculates the coupling potential. We should note, however, that in double folding calculations the coupling potential is calculated up to first order for both nuclear and Coulomb interactions.

2.2.7 Solution of the Schrodinger Equation for the $^{16}O +^{238} U$ System

Eq. 2.23 is the Schrodinger equation for our system. The tunnelling transmission probabilities can be found from ϕ_I^J functions which are obtained by solving 2.23. 2.23 is a set of second order differential equations and in this set there are as many equations as the number of excited states that is included in the coupling process. The CCFULL program which is briefly mentioned above is written to

solve this coupled channels equations. The program includes the iso-centrifugal approximation to reduce the dimension of the couplings. It firstly calculates the coupling potential to full order for Woods-Saxon case and to first order for double folding case, and by using this potential solves the coupled channels equation. The description of the program and information about how it works can be found [38].

CHAPTER 3

RESULTS AND CONCLUSION

3.1 Results

The fusion cross section can be obtained by running the CCFULL program for each potential type. We obtained the cross section with the use of Woods-Saxon potential by running the original CCFULL code. If Double Folding procedure is used instead of the Woods-Saxon potential then the modified CCFULL program must be run to obtain the cross section. The necessary constants which are given as input to the program, are given in Appendix D for both Woods-Saxon and Double Folding cases.

Plots of the obtained cross sections are shown in Fig. 3.1. In this graph four different cross sections are plotted, one for Woods-Saxon, one for Double Folding, one for the experimental result and one for the bare potential without coupling case. The experimental result for $^{16}O +^{238} U$ system is taken from [40].

3.2 Discussion

We have studied the effects of nuclear intrinsic degrees of freedom on heavy ion fusion reactions. If we consider that for our $O + U$ system the Coulomb barrier is between 83 MeV and 86 MeV, we can see from our results that below

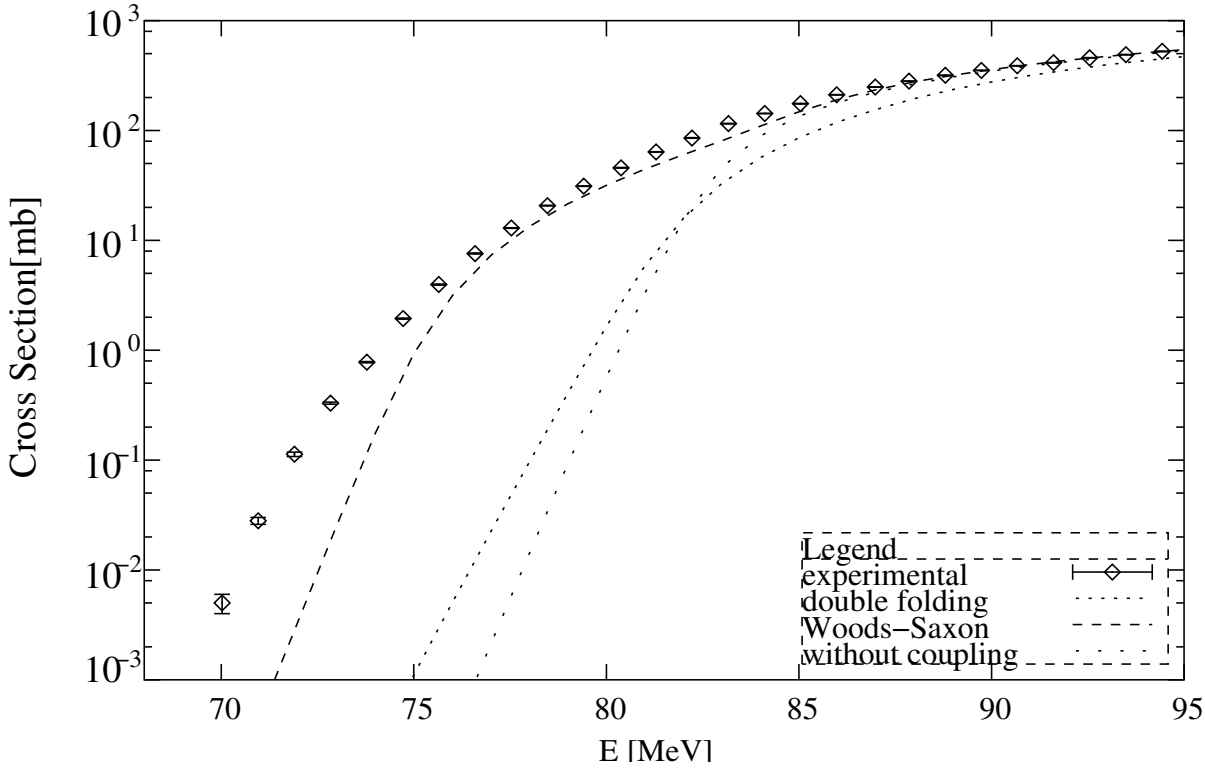

Figure 3.1: Cross section for theoretical calculations and experimental data.

the Coulomb barrier we get closer to the experimental cross section when we compare to the bare potential case. This shows that contrary to most complex physical systems multidimensional quantum tunnelling enhances the tunnelling probability and improves the agreement between experimental and theoretical cross sections. This result has two important interpretations. (I) The intrinsic structure of complex nuclei changes the result and accordingly we can design heavy-ion fusion experiments that give information about the nuclear structure, (II) With this result we have a theory that gives correct predictions both at sub-barrier and above-barrier energies. A complete theory of fusion may give us a chance to find ways of preparing heavy-ion systems which have high probability of fusing at sub-barrier energies. This would definitely be very helpful in obtaining

the predicted superheavy elements. Also energy extraction from fusion reactions would be possible by the same reasoning.

Since we wanted to obtain a theoretical model that mostly resembles the real situation, we used two different forms of potential for calculations. From the results, it is seen that use of Woods-Saxon type potential is more appropriate, at least for heavy ion calculations. However, we should keep in mind that the calculation performed for the double folding potential is calculated only up to first order in β_2, higher order β_λ coefficients are taken to be zero. On the other hand Woods-Saxon potential is calculated by using all orders having contribution to the cross section. When we include β_λ in our calculations we deviate our system from the simple one dimensional case. So Woods-Saxon results are more realistic in this work. The difficulty of the integrals appearing in double folding calculations makes it hard to obtain higher order terms. However, studies are carried on to obtain the full order results in double folding also. To make comparison between the two potentials it is better to wait until the full order result is obtained for double folding case.

In the problem treated in this thesis we only assumed the pure rotational excitation of the ^{238}U nucleus. In practice there are other forms of excitations of course. In the preceding chapters we mentioned that high energy single particle states does not contribute to the result. This is shown by recent studies on the subject [25]. Nevertheless, it is known that vibrational excitations combined with the rotational states affect the fusion cross section. ^{238}U nucleus may have pure rotational excitations, pure vibrational excitations or the combination of

these two. So, if a more exact treatment is done by including these states, the interpretation of the multidimensional tunnelling modelling may be done more consistently.

REFERENCES

[1] Iachello, F., and Arima A., 1987, The Interacting Boson Model (Cambridge University, Cambridge, England).

[2] Balantekin, A.B., Takigawa N., Rev. Mod. Phys., 70 (77) 1998, Quantum tunneling in nuclear fusion.

[3] Vaz, L. C., J. M. Alexander, and Satchler G. R., 1981, Phys. Rep. C 69, 373.

[4] Beckerman, M., 1988, Rep. Prog. Phys. 51, 1047.

[5] Vandenbosch, R., 1992, Annu. Rev. Nucl. Part. Sci. 42, 447.

[6] Balantekin, A. B., Koonin S. E., and Negele J. W., 1983, Phys. Rev. C 28, 1565.

[7] Reisdorf, W., 1994, J. Phys. G 20, 1297.

[8] Stefanini, A. M., 1994, in Proceedings of the International Workshop on "Heavy-Ion Fusion: Exploring the Variety of Nuclear Properties," Padua, Italy, May 25-27, (World Scientific, Singapore).

[9] Wong, C. Y., 1973, Phys. Rev. Lett. 31, 766.

[10] Vaz L. C., and J.M. Alexander, 1974, Phys. Rev. C 10, 464.

[11] Stokstad, R. G., Eisen Y., Kaplanis S., Pelte D., Smilansky U., and Tserruya I., 1978, Phys Rev. Lett.41, 465 ; 1980, Phys. Rev. C 21, 2427.

[12] Reisdorf, W., et al., 1982, Phys. Rev. Lett., 49, 1811.

[13] Reisdorf, W., et al., 1985, Nucl. Phys., A438, 212.

[14] Thompson, I. J., Nagarajan M. A., J. S. Lilley, and Fulton B. R., 1985, Phys. Lett. B 157, 250.

[15] Stefanini, A. M., Wu J., et al., 1990, Phys. Lett. B 240, 306.

[16] Kapur, P.L., Peierls R., 1937, Proc. Roy. Soc., A163, 606.

[17] Brink, D. M., Nemesand M. C., Vautherin D., 1983, Ann. Phys. (N.Y.) 147, 171.

[18] Schmid, A., 1986, Ann. Phys. (N.Y.) 170, 333.

[19] Takada, S., H. Nakamura, 1994, J. Chem. Phys. 100, 98.

[20] Caldeira, A. O., and Leggett A. J., 1983, Ann. Phys. (N.Y.) 149, 374.

[21] Satoh, T., et al., 1994, Physica B197, 397.

[22] Karlsson, E., et al., 1995, Phys. Rev. B52, 6417.

[23] Vilenkin, A., 1998, Phys. Rev. D37, 888.

[24] Rumin, T., 1998, Sub-Barrier Fusion of Deformed Nuclei, Ph.D. Thesis, Department of Physics, Tohoku University, Japan.

[25] Hagino, K., N. Takigawa, M. Dasgupta, D.J. Hinde, J.R. Leigh, 1997, Phys. Rev. Lett. 79, 2094.

[26] Moddy, K., LLNL http://www.llnl.gov/str/JanFeb02/Moody.html.

[27] Brink, D. M., and U. Smilansky, 1983, Nucl. Phys. A 405, 301.

[28] Brink, D. M., 1985a, Semi-Classical Methods for Nucleus-Nucleus Scattering (Cambridge University, Cambridge, England).

[29] Hill, D. L., and J. A. Wheeler, 1953, Phys. Rev. 89, 1102.

[30] http://nrv.jinr.ru/nrv/webnrv/fusion/.

[31] McGuire, P., D.J. Kouri, 1974, J. Chem. Phys. 60, 2488.

[32] Mclenithan, K., and D. Secrest, 1984, J. Chem. Phys. 80, 2480.

[33] Balantekin, A. B., et al, 1986, Phys. Rev. C34, 894.

[34] Tanimura, O., 1987, Phys. Rev. C35, 1600.

[35] Takigawa, N., T. Masamoto, T. Takehi, T. Rumin, to be published.

[36] Satchler, G.R., W.G. Love, 1979, Phys. Rep. 55, 183.

[37] Jeukenne, J.P., A. Lejeune , C. Maltaux, 1977, Phys. Rev. C16, 80.

[38] Hagino K., N. Rowley, A.T. Kruppa, 1999, Computer Physics Communications 123 143-152.

[39] Kermode M. W., N. Rowley, 1993, Phys. Rev. C 48 2326.

[40] Hinde, D.J., et al, Phys. Rev. C3, 53 (1290).

[41] Bohr, A., Mottelson B. R., 1975, Nuclear structure, (Published by New York, W. A. Benjamin).

APPENDIX A

NUCLEAR SURFACE DEFORMATIONS

The behavior of nuclei with proton or neutron numbers far away from the magic numbers of the shell model can be described by using unified model proposed by Rainwater and Bohr-Mottelson [41]. According to this model nuclei with excess nucleons are deformed in shape and they have collective degrees of freedom as well as single-particle states described by the shell model. These collective states may be in the form of rotational or vibrational excitations. Depending on the structure of the nuclei two types may be observed at the same time. Normally these collective motions create new quantum states and new energy levels for such nuclei. One important property of these collective states is that they have lower energy than the single particle states.

In Fig. A.1 the shape of a deformed nucleus and the corresponding angular momentum vectors are shown. If the nucleus is a symmetrical ellipsoid then we can choose the symmetry axis along the z axis of the body-fixed coordinate system. Accordingly the rotational angular momentum $\vec{R}$ can not have components along this direction. The sum of the single-particle orbital and spin angular momentum of the nucleus is denoted by $\vec{J}$ in Fig. A.1 and the total angular

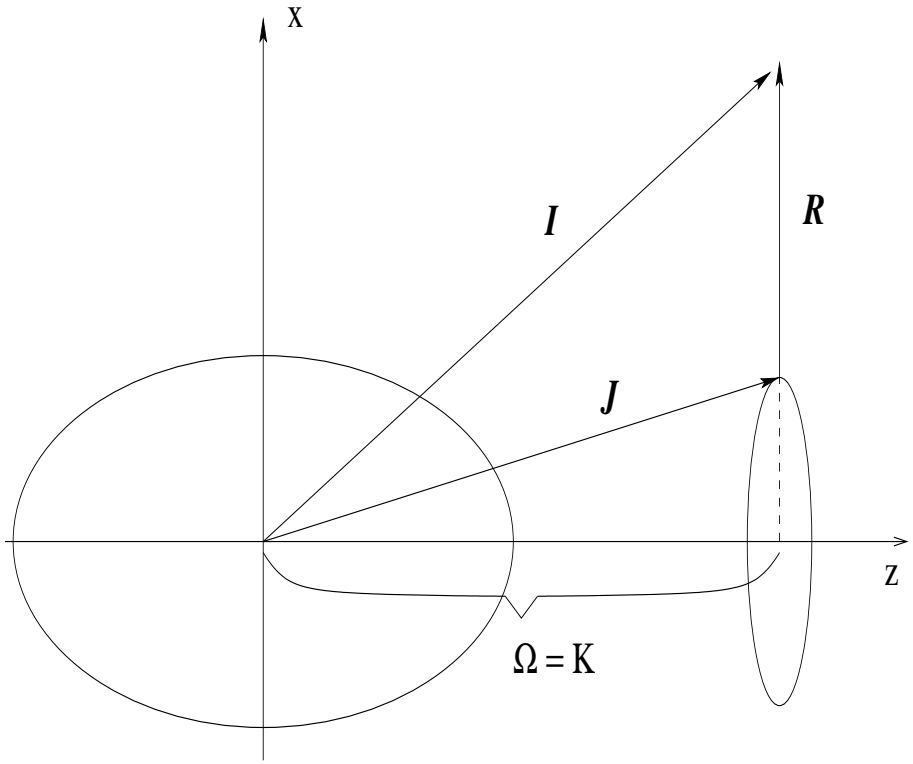

Figure A.1: Possible rotations and the corresponding angular momentum vectors for a deformed nucleus.

momentum of the deformed nuclei is given by

$$\vec{I} = \vec{R} + \vec{J}. \tag{A.1}$$

$\vec{J}$ may have component along the symmetry axis and this component is denoted by K. If we consider $even - even$ nucleus only, then we take $\vec{J}$ as zero because nucleons in such nuclei place themselves in zero spin and angular momentum configurations. Accordingly $K = 0$ and along the body fixed z axis there is no angular momentum. $\vec{I}$ for such a nucleus is given by

$$I^2 = I(I+1)\hbar^2. \tag{A.2}$$

Wave function of the even-even nuclei must be symmetric with respect to a plane perpendicular to the symmetry axis. So for nuclei with $K = 0$, the angular

momentum number I can have even values only:

$$I = 0, 2, 4, \ldots.$$

In the unified model radius of the deformed nuclei can be given by an expansion of the form

$$R(\Omega) = R_T \left(1 + \sum_{\lambda \neq 0} \sum_{\mu=-\lambda}^{\lambda} \alpha_{\lambda\mu} Y^*_{\lambda\mu}(\Omega) \right). \tag{A.3}$$

This form is valid in an arbitrary frame. We can switch to the body-fixed coordinate system by transforming $\alpha_{\lambda\mu}$ and $Y^*_{\lambda\mu}(\Omega)$ functions to that frame by using

$$\begin{aligned} Y^*_{\lambda\mu}(\Omega) &= \sum_{\mu'} D^{\lambda}_{\mu'\mu}(\omega) Y_{\lambda\mu'}(\Omega') \\ \alpha_{\lambda\mu} &= \sum_{\mu'} D^{\lambda}_{\mu\mu'}(\omega) a_{\lambda\mu'}. \end{aligned} \tag{A.4}$$

Following Bohr and Mottelson [**?**] we can describe the deformation by using a, β and γ. For the quadruple deformation a are given by

$$\begin{aligned} a_{2,0} &= \beta \cos\gamma \\ a_{2,2} = a_{2,-2} &= \frac{1}{\sqrt{2}} \beta \sin\gamma \\ a_{2,1} = a_{2,-1} &= 0. \end{aligned} \tag{A.5}$$

For a permanently deformed symmetrical ellipsoid nucleus, a and α are given by

$$\begin{aligned} a_{\lambda\mu'} &= \beta_\lambda \delta_{\mu 0} \\ \alpha_{\lambda\mu} &= D^{\lambda}_{\mu\mu'}(\omega) \beta_\lambda. \end{aligned} \tag{A.6}$$

Then the radius of a deformed nucleus in the body-fixed coordinate system is given by

$$R(\Omega) = R_T \left(1 + \sum_{\lambda} \beta_\lambda Y^*_{\lambda 0}(\Omega) \right). \tag{A.7}$$

In this thesis we need to deal with the rotational states of ^{238}U nucleus with $K = 0$. So the analysis above can be used to describe ^{238}U.

APPENDIX B

SOLUTION OF THE COULOMB INTEGRAL

Integral in Eq. 2.41 can be evaluated as follows. Inserting Eq. 2.42 for $\frac{1}{|\vec{r}-\vec{r}'|}$ we rewrite 2.41 as

$$V_C = eZ_P\rho_C \sum_{\lambda\mu} \frac{4\pi}{2\lambda+1} \int d\Omega' Y^*_{\lambda\mu}(\Omega') Y_{\lambda\mu}(\Omega) \int_0^{R_\beta} dr' r'^2 \frac{r'^{\lambda+2}}{r^{\lambda+1}} \tag{B.1}$$

where R_β is given by

$$R_\beta = R_{T0}\left\{1 + \sum_{lm} \alpha^*_{lm} Y_{lm}(\Omega')\right\} = R_{T0} + \Delta. \tag{B.2}$$

Using the well known mathematical expression for small deviations

$$F(z+\varepsilon) = \int_0^{z+\varepsilon} f(u)du = F(z) + \varepsilon \frac{df}{dz} + \dots \tag{B.3}$$

we can evaluate the r' integral in Eq. B.1

$$\int_0^{R_\beta} dr' r'^2 r'^{\lambda+2} \simeq \int_0^{R_{T0}} dr' r'^2 r'^{\lambda+2} + \Delta r'^{\lambda+2}|_{r'=R_{T0}}. \tag{B.4}$$

When the limits of integrations are inserted the result is found to be

$$\int_0^{R_\beta} dr' r'^2 r'^{\lambda+2} = \frac{R_{T0}^{\lambda+3}}{\lambda+3} + R_{T0}^{\lambda+3} \sum_{lm} \alpha^*_{lm} Y_{lm}(\Omega'). \tag{B.5}$$

If we insert this result into Eq. B.1 we have

$$\begin{aligned} V_C = eZ_P\rho_C \quad & \textstyle\sum_{\lambda\mu} \quad \frac{4\pi}{2\lambda+1} \frac{1}{r^{\lambda+1}} Y_{\lambda\mu}(\Omega) \left\{ \frac{R_{T0}^{\lambda+3}}{\lambda+3} \sqrt{4\pi} \int d\Omega' Y^*_{\lambda\mu}(\Omega') Y_{00}(\Omega') \right. \\ & + \quad \left. R_{T0}^{\lambda+3} \sum_{lm} \alpha^*_{lm} \int d\Omega' Y^*_{\lambda\mu}(\Omega') Y_{lm}(\Omega') \right\}. \end{aligned} \tag{B.6}$$

Remembering the orthogonality property of spherical harmonics,

$$\int d\Omega' Y^*_{\lambda\mu}(\Omega') Y_{lm}(\Omega') = \delta_{\lambda l}\delta_{\mu m} \tag{B.7}$$

and inserting the value of ρ_c we can write V_c as

$$V_C = \frac{e^2 Z_P Z_T}{r} + \sum_{\lambda\mu} \frac{3 Z_P Z_T}{2\lambda+1} \frac{R_{T0}}{r^{\lambda+1}} \alpha^*_{\lambda\mu} Y_{\lambda\mu}(\Omega'). \tag{B.8}$$

Transforming the spherical harmonics to the body-fixed coordinate system the final form of V_c is obtained as

$$V_C = \frac{e^2 Z_P Z_T}{r} + \sum_{\lambda even} \frac{3 Z_P Z_T}{2\lambda+1} \frac{R_{T0}}{r^{\lambda+1}} \beta_\lambda Y_{\lambda 0}(\theta). \tag{B.9}$$

APPENDIX C

SOLUTIONS OF THE DOUBLE FOLDING INTEGRALS

We need to solve the integrals in Eq. 2.53 for $\lambda = 0$ and $\lambda = 2$ for both Coulomb and nuclear interactions. Only the solution for $\lambda = 0$ will be given here. The other solutions can be performed by using the same methods.

For bare Coulomb interaction, that is for $\lambda = 0$, the $V_0(r)$ integral has the form

$$V_0(r) = 8 \int_0^\infty dk \frac{j_0(kr) j_1(kR_p) j_1(kR_{T0})}{(1 + k^2 a_p^2)(1 + k^2 a_T^2)} \widetilde{v}(k). \tag{C.1}$$

If we put the value of $\widetilde{v}(k)$ for Coulomb interaction which is given by

$$\widetilde{v}(k) = \frac{4\pi e^2}{k^2} \tag{C.2}$$

and use the definition of spherical Bessel functions

$$j_\lambda(kr) = \left(\frac{d}{dr}\right)^\lambda \frac{1}{r} \frac{\sin kr}{k^{\lambda+1}} \tag{C.3}$$

for $\lambda = 0$, we transform C.1 into

$$\frac{i}{r} \left(\frac{d}{dr_P} \frac{1}{r_p}\right) \left(\frac{d}{dr_T} \frac{1}{dr_T}\right) \int_{-\infty}^{\infty} \frac{dk}{k^7} \frac{N}{(1 + k^2 {a_P}^2)(1 + k^2 {a_T}^2)} \tag{C.4}$$

where N is given by

$$N = \exp[ik(r+r_P+r_T)]+\exp[ik(r-r_P+r_T)]+\exp[ik(r+r_P-r_T)]+\exp[ik(r-r_P-r_T)]. \tag{C.5}$$

Setting

$$\begin{aligned} r + r_P + r_T &= t \qquad\qquad r - r_P + r_T = s \\ r + r_P - r_T &= u \qquad\qquad r - r_P - r_T = v \end{aligned} \tag{C.6}$$

we have an integral of the form

$$\frac{i}{r}\left(\frac{d}{dr_P}\frac{1}{r_p}\right)\left(\frac{d}{dr_T}\frac{1}{dr_T}\right)\int_{-\infty}^{\infty}\frac{dk}{k^7}\frac{\{\exp[ikt]+\exp[iks]+\exp[iku]+\exp[ikv]\}}{(1+k^2{a_P}^2)(1+k^2{a_T}^2)}. \tag{C.7}$$

We can put this integral even simpler form by use of two simple algebraic equalities

$$\begin{aligned} \frac{1}{(1+k^2{a_P}^2)(1+k^2{a_T}^2)} &= \frac{a_P^2}{a_P^2-a_T^2}\frac{1}{(1+k^2{a_P}^2)}+\frac{a_T^2}{a_T^2-a_P^2}\frac{1}{(1+k^2{a_T}^2)} \\ \frac{1}{k^7}\frac{1}{(1+k^2{a_P}^2)} &= \frac{1}{k^7}-\frac{a_p^2}{k^5}+\frac{a_p^4}{k^3}-\frac{a_P^6}{k(1+k^2{a_P}^2)}. \end{aligned} \tag{C.8}$$

Then our integral becomes

$$\begin{aligned} & \frac{i}{r}\left(\frac{d}{dr_P}\frac{1}{r_p}\right)\left(\frac{d}{dr_T}\frac{1}{dr_T}\right) \\ \times\ & \left\{C_P\left(\int_{-\infty}^{\infty}\frac{Ndk}{k^7}+\int_{-\infty}^{\infty}\frac{a_P^2Ndk}{k^5}+\int_{-\infty}^{\infty}\frac{a_P^4Ndk}{k^3}+\int_{-\infty}^{\infty}\frac{a_P^6Ndk}{k(1+k^2{a_P}^2)}\right)\right. \\ +\ & \left. C_T\left(\int_{-\infty}^{\infty}\frac{Ndk}{k^7}+\int_{-\infty}^{\infty}\frac{a_T^2Ndk}{k^5}+\int_{-\infty}^{\infty}\frac{a_T^4Ndk}{k^3}+\int_{-\infty}^{\infty}\frac{a_T^6Ndk}{k(1+k^2{a_T}^2)}\right)\right\} \end{aligned} \tag{C.9}$$

where

$$\begin{aligned} C_P &= \frac{a_P^2}{a_P^2-a_T^2} \\ C_T &= \frac{a_T^2}{a_T^2-a_P^2}. \end{aligned} \tag{C.10}$$

So we need to obtain the result of the integrals

$$\int_{-\infty}^{\infty}\frac{\exp[ikt]dk}{k^n}$$

$$\int_{-\infty}^{\infty} \frac{Ndk}{k(1+k^2{a_P}^2)}. \tag{C.11}$$

These integrals can be handled easily by using the contour integration methods of complex calculus. The results are found to be

$$\begin{aligned} \int_{-\infty}^{\infty} \frac{\exp[ikt]dk}{k^n} &= (i\pi)\frac{(it)^{n-1}}{(n-1)!} \\ \int_{-\infty}^{\infty} \frac{\exp[ikt]dk}{k(1+k^2{a_P}^2)} &= (i\pi)\left(1-\frac{a_P}{e^{t/a_P}}\right). \end{aligned} \tag{C.12}$$

Inserting the results into the potential integral we can find the result for the bare Coulomb interaction. Arranging all the terms the result is given by

$$V_0^C(r) = \frac{9e^2}{4\pi}\frac{A_T A_P}{R_{T0}R_P}\left\{C_P I_P + C_T I_T\right\} \tag{C.13}$$

where I_P is given by

$$\begin{aligned} I_P &= \frac{1}{rR_P^2R_T^2}\left[\frac{\pi}{6!}(t^6-S^6-u^6+v^6)\right. \\ &+ \frac{\pi a_P^2}{4!}(t^4-S^4-u^4+v^4)+\frac{\pi a_P^4}{2!}(t^2-S^2-u^2+v^2) \\ &+ \left.\frac{\pi a_P^7}{1!}(\exp[-t/a_P]-\exp[-s/a_P]-\exp[-u/a_P]+\exp[-v/a_P])\right] \\ &- \frac{1}{rR_PR_T^2}\left[\frac{\pi}{5!}(t^5+S^5-u^5-v^5)\right. \\ &+ \frac{\pi a_P^2}{3!}(t^3+S^3-u^3-v^3)+\pi a_P^4(t+S-u-v) \\ &+ \left.\frac{\pi a_P^6}{1!}(-\exp[-t/a_P]-\exp[-s/a_P]+\exp[-u/a_P]+\exp[-v/a_P])\right] \\ &- \frac{1}{rR_P^2R_T}\left[\frac{\pi}{5!}(t^5-S^5+u^5-v^5)\right. \\ &+ \frac{\pi a_P^2}{3!}(t^3-S^3-u^3+v^3)+\pi a_P^4(t-s+u-v) \\ &+ \left.\frac{\pi a_P^6}{1!}(-\exp[-t/a_P]+\exp[-s/a_P]-\exp[-u/a_P]+\exp[-v/a_P])\right] \\ &+ \frac{1}{rR_PR_T}\left[\frac{\pi}{4!}(t^4+S^4+u^4+v^4)\right. \end{aligned}$$

$$
\begin{aligned}
&+ \quad \frac{\pi a_P^2}{2!}(t^2+S^2+u^2+v^2) + 4\pi a_P^4 \\
&+ \quad \frac{\pi a_P^5}{1!}(\exp[-t/a_P]+\exp[-s/a_P]+\exp[-u/a_P]+\exp[-v/a_P])\Bigg] .
\end{aligned}
\tag{C.14}
$$

In Eq. C.13, I_T is obtained by inserting a_T instead of a_P in the I_P expression.

The other coefficients for the zeroth and first order terms of the coupling potential are given by

$$
\begin{aligned}
V_0^N(r) &= \frac{9V_0a_N^3}{4\pi}\frac{A_TA_P}{R_{T0}R_P}\{D_PJ_P + D_TJ_T + D_NJ_N\} \\
V_2^C(r) &= \frac{9e^2}{4\pi}\frac{A_TA_P}{R_{T0}R_P}\{C_PI_{2P} + C_TI_{2T}\} \\
V_2^N(r) &= \frac{9V_0a_N^3}{4\pi}\frac{A_TA_P}{R_{T0}R_P}\{D_PJ_{2P} + D_TJ_{2T} + D_NJ_{2N}\}
\end{aligned}
\tag{C.15}
$$

where

$$
\begin{aligned}
D_P &= \frac{a_P^4}{(a_P^2-a_n^2)(a_P^2-a_T^2)} \\
D_T &= \frac{a_T^4}{(a_T^2-a_n^2)(a_T^2-a_P^2)} \\
D_n &= \frac{a_n^4}{(a_n^2-a_P^2)(a_n^2-a_T^2)}.
\end{aligned}
\tag{C.16}
$$

In Eq. C.15 I_i and J_i terms have the same form as I_P in the $V_0^C(r)$ solution. So they can be evaluated similarly.

APPENDIX D

CONSTANTS

Below the constants used in this thesis are given in tabular form. The first table gives the atomic and proton numbers of Oxygen and Uranium. In the following tables constants for Woods-Saxon and for double folding calculations are given. As it is seen from the tables, the same constants have different values for different procedures. In the second and third tables E_{R2} is the energy of the first rotationally excited state of Uranium.

Nucleus	A	Z
Oxygen (Projectile)	16	8
Uranium (Target)	238	92

Table D.1: Proton and atomic numbers

a_0 (fm)	r_0 (fm)	V_0 (MeV)	β_2	β_4	β_6	E_{R2}(MeV)
0.81	1.26	349	0.26	0.06	0.01	0.044

Table D.2: Constants used in the Woods-Saxon Calculations

	a_P (fm)	a_T (fm)	R_P (MeV)	R_{T0}	β_2	β_4	E_{R2}(MeV)
Coulomb Int.	0.5782	0.5944	2.7638	7.1766	0.262	0	0.044
Nuclear Int.	0.6423	0.7568	2.5938	7.0066	0.262	0	0.044

Table D.3: Constants used in the Double Folding Calculations for ^{238}U